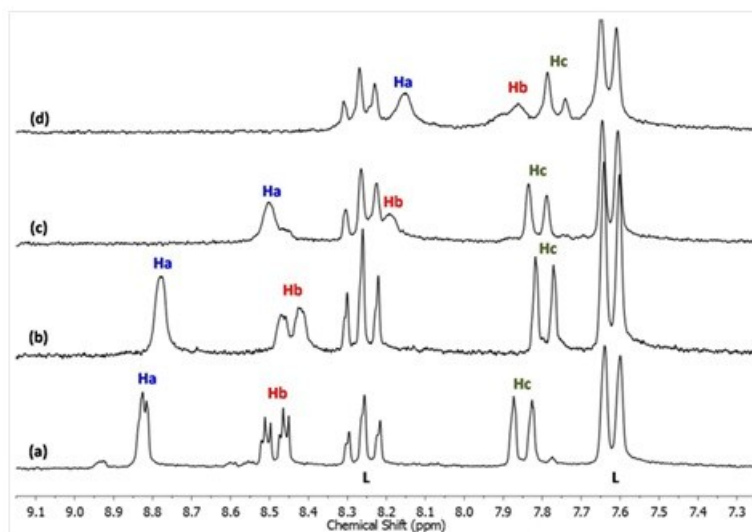


## Supramolecular Phosphate Transfer Catalysis by Pillar[5]arene

Daiane G. Liz, Alex M. Manfredi, Michelle Medeiros, Rodrigo Montecinos, Borja Gómez-González, Luis Garcia-Rio and Faruk Nome

### Supporting Information Section

#### 1. DNPP NMR spectra as a function of P5A concentration



**Figure S-1.**  $^1\text{H}$  NMR spectra ( $\text{D}_2\text{O}$ , 298 K, 200 MHz) of DNPP (19.3 mM) in the presence of increasing concentrations of P5A (mM): (a) 0.00, (b) 0.7, (c) 3.5 and (d) 16 mM. The signals marked as L correspond to the 2,6-lutidinium counter ion.

## 2. Molecular Dynamic calculations for the 1:2 host:guest complex

Experimental conditions with DNPP is in large excess over P5A allow the formation of a supramolecular complex between 2 molecules of DNPP and 1 molecule of pillar[5]arene. In order to speed the calculation, the initial configuration corresponds to P5A with 2 molecules of DNPP inside the cavity. The model rapidly evolved to a structure where one DNPP molecule is maintained inside of the cavity, forming an internal complex. The second molecule is located on the opposite side of the cavity, interacting with the ammonium group and thus forming an external complex (Figure S-2). Distances between the center of the P5A cavity and the carbon in position-4 of each DNPP molecule are stable as a function of calculation time evidencing the stability of the internal and external complexes. According to these results, the samples of DNPP with an excess of pillar[5]arene interact favouring a preferential structure 1:1 through the formation of an internal complex.

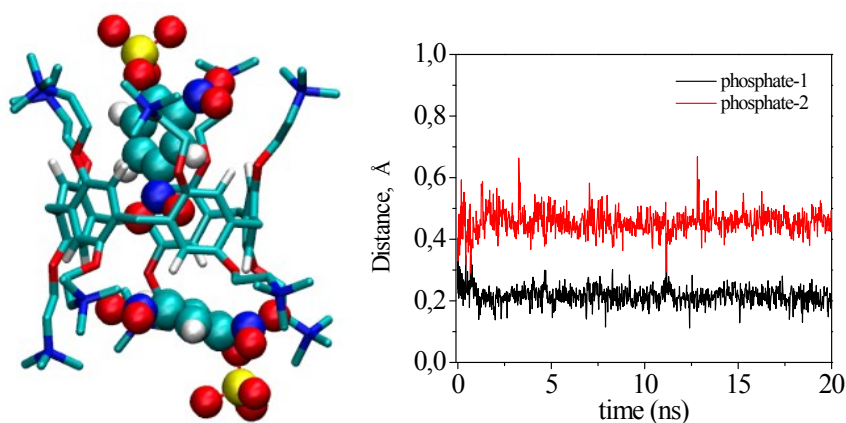


**Figure S-2.** A Snapshot of 2:1 host-guest complex, P5A is represented in sticks (orange), DNPP in CPK, with carbons in cyan, hydrogens in white, nitrogens in blue and oxygens in red. For simplicity water molecules and ions are not shown. B. Distance between the center of the P5A cavity and the carbon in position-4 for each DNPP, as a function of calculation time.

### 3. Treatment of the kinetic data

The rate vs. host concentration profile for DNPP hydrolysis show that the rate constant increases with the concentration of P5A, reaching a plateau. The observed rate constant increases almost ten-fold on increasing the pillararene concentration, reaching a limiting value for [P5A]>0.002M. The observed catalytic effect can be explained by considering the incorporation of the DNPP dianion in the supramolecular cavity, so that the reaction takes place simultaneously in both bulk water,  $k_{D,w}$ , and the cavity of pillararene,  $k_{D,P5A}$ . The observed rate constant is the sum of the rate constants in the two environments weighted by the molar fractions  $X_{D,w}$  and  $X_{D,P5A}$  of monoester dianion in each.

$$k_{obs} = k_{D,w}X_{D,w} + k_{D,P5A}X_{D,P5A} \quad (1)$$

$$X_{D,w} = \frac{1}{1 + K_{ass,D}[P5A]} \quad \text{and} \quad X_{D,P5A} = \frac{K_{ass,D}[P5A]}{1 + K_{ass,D}[P5A]} \quad (2)$$

The kinetic results shown in Figure 4 are consistent with Scheme 2, which summarises the reactions of DNPP in the presence and absence of pillar[5]arene. By considering that monoester hydrolysis takes place through four simultaneous pathways: (i) monoanion in water,  $k_{M,w}$ , (ii) monoanion bound to the pillararene,  $k_{M,P5A}$ , (iii) dianion in water,  $k_{D,w}$ , and (iv) dianion bound in the pillararene cavity,  $k_{D,P5A}$ . Equation (3) assumes  $k_{obs}$  to be the sum of the individual rate constants weighted by the corresponding monoester mole fractions.

$$k_{obs} = k_{M,w}X_{M,w} + k_{D,w}X_{D,w} + k_{M,P5A}X_{M,P5A} + k_{D,P5A}X_{D,P5A} \quad (3)$$

$$X_{M,w} = \frac{[H^+]}{(K_{ass,M}[P5A] + 1)[H^+] + K_{a,w}(1 + K_{ass,D}[P5A])} \quad (4)$$

$$X_{M,P5A} = \frac{K_{ass,M}[P5A][H^+]}{(K_{ass,M}[P5A] + 1)[H^+] + K_{a,w}(1 + K_{ass,D}[P5A])} \quad (5)$$

$$X_{D,w} = \frac{K_{a,w}}{(K_{ass,M}[P5A] + 1)[H^+] + K_{a,w}(1 + K_{ass,D}[P5A])} \quad (6)$$

## Experimental

**Materials.** Inorganic salts were of analytical grade and were used without further purification. Liquid reagents were purified by distillation. The phosphate ester DNPP was prepared by standard methods from POCl<sub>3</sub>, as described previously<sup>1</sup>. The cationic water-soluble pillar[5]arene, AP5, was synthesized according to a literature procedure.<sup>2</sup>

**Kinetics.** Reactions of DNPP were followed spectrophotometrically by monitoring the appearance of 2,4-dinitrophenolate (DNP) at 400 nm. Reactions were started by adding 15 μL of M stock solutions of the substrate in acetonitrile to 3 mL of aqueous solutions to give a final concentration of DNPP of 5.0 10<sup>-5</sup> M. The temperatures of reaction solutions in quartz cuvettes were controlled with a thermostated water-jacketed cell holder. Absorbance versus time data were stored directly on a microcomputer, and observed first-order rate constants, *k*<sub>obs</sub>, calculated using an iterative least-squares program; correlation coefficients were > 0.999 for all kinetic runs. The pH was maintained with 0.01 M buffers of CH<sub>2</sub>ClCOOH (pH 2-3), HCOOH (pH 3-4.5), CH<sub>3</sub>COOH (pH 4-5.5), NaH<sub>2</sub>PO<sub>4</sub> (pH 5.5-6.0), Bis-Tris (pH=6-7); Tris (pH=7-9) and KHCO<sub>3</sub> (pH 9-11).

**NMR Spectrometry.** <sup>1</sup>H spectra were monitored on a spectrometer (400 and 200 MHz) at 25°C, in D<sub>2</sub>O. <sup>1</sup>H chemical shifts are referred to internal sodium 3-(trimethylsilyl) propionate (TMSP). The chemical shifts were assigned by comparison with spectra of the pure compounds and data given in the literature.<sup>3</sup>

**Simulation Specifications.** Molecular Dynamics (MD) simulations were performed using the program package Gromacs version 4.6.5.<sup>4</sup> Pillar[5]arene and DNPP were built with parameters from GROMOS96 54A7<sup>5</sup> force field and solvated using the SPC/E water model.<sup>6</sup> Periodic boundary conditions were applied in all three dimensions and all the simulations were performed in the isothermic-isobaric ensemble. The temperature was maintained at 300 K using v-rescale algorithm with pillar[5]arene\_DNPP and ions\_water groups coupled independently with a coupling time constant of 0.1 ps. The pressure was maintained at 1 bar using Berendsen barostat with a coupling time constant of 1.0 ps.<sup>7</sup> LINCS algorithm<sup>8</sup> was used to constrain the bond lengths of the pillar[5]arene and DNPP and SETTLE<sup>9</sup> to restrict the structure of the water molecules. A 1.2 nm cut-off was used for the Van der Waals interactions. Long range electrostatic interactions were calculated using particle mesh Ewald algorithm (PME).<sup>10</sup> A time step of 2 fs was used throughout the simulations. The neighbor list was updated every 10 time steps. Both systems were equilibrated by 300 ps. Trajectories of 50 ns were calculated for each systems.

## Notes and references

- 1 E. S. Orth, P. L. F. da Silva, R. S. Mello, C. A. Bunton, H. M. S. Milagre, M. N. Eberlin, H. D. Fiedler, F. Nome, *J. Org. Chem.*, 2009, **74**, 5011.)
- 2 Y. Ma, X. Ji, F. Xiang, X. Chi, C. Han, J. He, Z. Abliz, W. Chen, F. Huang, *Chem. Commun.*, 2011, **47**, 12340-12342.
- 3 J. B. Domingos, E. Longhinotti, T. A. S. Brandão, L. S. Santos, M. N. Eberlin, C. A. Bunton, F. Nome, *J. Org. Chem.*, 2004, **69**, 7898.
- 4 S. Pronk, S. Pl, R. Schulz, P. Larsson, P. Bjelkmar, R. Apostolov, M. R. Shirts, J. C. Smith, P. M. Kasson, D. van der Spoel, B. Hess, E. Lindahl, *Bioinformatics*, 2013, **29**, 845–854.
- 5 N. Schmid, A. Eichenberger, A. Choutko, S. Riniker, M. Winger, A. Mark, W. van Gunsteren, *European Biophysics Journal*, 2011, **40**, 843–856.
- 6 H. J. C. Berendsen, J. R. Grigera, and T. P. Straatsma, *J. Phys. Chem.*, 1987, **91**, 6269-6271
- 7 H. J. C. Berendsen, J. P. M. Postma, W. F. van Gunsteren, A. DiNola, J. R. J. Haak, *Chem. Phys.*, 1984, **81**, 3684-3690.
- 8 B. Hess, H. Bekker, H. J. C. Berendsen, J. G. E. M. Fraaije, *J. Comp. Chem.*, 1997, **18**, 1463-1472.
- 9 S. Miyamoto, P. A. Kollman, *J. Comput. Chem.*, 1992, **13**, 952-962.
- 10 T. Darden, D. York, L. Pedersen, *J. Chem. Phys.*, 1993, **98**, 10089-10092.